Journal of Nuclear Medicine, published on April 13, 2020 as doi:10.2967/jnumed.120.241976

PET imaging of phosphodiesterase-4 identifies affected dysplastic bone in McCune-Albright syndrome, a genetic mosaic disorder

Lora D. Weidner[1]*, Yuichi Wakabayashi[1]*, Louise A. Stolz[1], Michael T. Collins[2], Lori Guthrie[2], Milalynn Victorino[1], Joyce Chung[3], William Miller[1], Sami S. Zoghbi[1], Victor W. Pike[1], Masahiro Fujita[1], Robert B. Innis[1†], and Alison M. Boyce[2†]

[1]Molecular Imaging Branch, National Institute of Mental Health, NIH, Bethesda, MD
[2]Skeletal Disorders and Mineral Homeostasis Section, National Institute of Dental and Craniofacial Research, NIH, Bethesda, MD
[3]Office of the Clinical Director, National Institute of Mental Health, NIH, Bethesda, MD

*† Authors contributed equally

For submission to *Journal of Nuclear Medicine* as a Full-Length Original Research Article

Correspondence
Yuichi Wakabayashi, M.D., Ph.D.
Molecular Imaging Branch
National Institute of Mental Health, National Institutes of Health
10 Center Drive, Rm. B1D43
Bethesda, MD 20892
Fax: +1 301 480 3610
Tel: +1 301 594 1371
Email; yuichi.wakabayashi@nih.gov

First Author
Lora D. Weidner, Ph.D., Postdoctoral Fellow
Molecular Imaging Branch
National Institute of Mental Health, National Institutes of Health
10 Center Drive, Rm. B1D43
Bethesda, MD 20892
Fax: +1 301 480 3610
Tel: +1 301 594 5721
Email: lora.deuitch@nih.gov

Financial Disclosures
This study was funded by the Intramural Research Programs of the National Institute of Mental Health (ZIAMH002852 and ZIAMH002793) and the National Institute of Dental and Craniofacial Research (ZIADE000649), National Institutes of Health.

Conflict of Interest
The authors have no conflicts of interest to disclose, financial or otherwise.

Manuscript information
Words: 4587
References: 34
Figures: 3
Tables: 2

Running Title: PDE4 PET in McCune-Albright syndrome

ABSTRACT

McCune-Albright syndrome (MAS) is a mosaic disorder arising from gain-of-function mutations in the *GNAS* gene, which encodes the 3′, 5′-cyclic adenosine monophosphate (cAMP) pathway-associated G-protein, $G_s\alpha$. Clinical manifestations of MAS in a given individual, including fibrous dysplasia, are determined by the timing and location of the *GNAS* mutation during embryogenesis, the tissues involved, and the role of $G_s\alpha$ in the affected tissues. The $G_s\alpha$ mutation results in dysregulation of the cAMP signaling cascade, leading to upregulation of phosphodiesterase type 4 (PDE4), which catalyzes the hydrolysis of cAMP. Increased cAMP levels have been found *in vitro* in both animal models of fibrous dysplasia and in cultured cells from individuals with MAS, but not in humans with fibrous dysplasia. Positron emission tomography (PET) imaging of PDE4 with ^{11}C-(*R*)-rolipram has been used successfully to study the *in vivo* activity of the cAMP cascade. To date, it remains unknown whether fibrous dysplasia and other symptoms of MAS, including neuropsychiatric impairments, are associated with increased PDE4 activity in humans.

Methods: ^{11}C-(*R*)-rolipram whole-body and brain PET scans were performed in six individuals with MAS (three for brain scans and six for whole-body scans) and nine healthy controls (seven for brain scans and six for whole-body scans).

Results: ^{11}C-(*R*)-rolipram binding correlated with known locations of fibrous dysplasia in the periphery of individuals with MAS; no uptake was observed in the bones of healthy controls. In peripheral organs and the brain, no difference in ^{11}C-(*R*)-rolipram uptake was noted between participants with MAS and healthy controls.

Conclusion: This study is the first to find evidence for increased cAMP activity in areas of fibrous dysplasia *in vivo*. No differences in brain uptake between MAS participants and controls

were detected, which could be due to several reasons, including the limited anatomic resolution of PET. Nevertheless, the results confirm the usefulness of PET scans with ^{11}C-(*R*)-rolipram to indirectly measure increased cAMP pathway activation in human disease.

Clinicaltrials.gov Identifier: NCT02743377 and NCT00001727

Keywords: Phosphodiesterase-4, McCune-Albright syndrome, cAMP, PET, ^{11}C-(*R*)-Rolipram

INTRODUCTION

McCune-Albright syndrome (MAS) is a rare genetic disorder arising from gain-of-function mutations in the *GNAS* gene (*1*). These mutations occur during the early embryogenesis of somatic cells and involve tissues derived from all three germ layers, which leads to a mosaic pattern of distribution. The *GNAS* mutation dysregulates the 3′, 5′-cyclic adenosine monophosphate (cAMP) pathway-associated G-protein, $G_s\alpha$, which leads to increased cAMP signaling. Increased cAMP, in turn, leads to the clinical manifestations of MAS, which include a variable combination of fibrous dysplasia of bone (including craniofacial dysplasia), café-au-lait skin pigmentation, and hyperfunctioning endocrinopathies such as precocious puberty. The specific features of any given individual are determined by the timing and location of the *GNAS* mutation during embryogenesis, the tissues involved, and the role of $G_s\alpha$ in the affected tissues (*2*).

Because cAMP is part of a signal transduction cascade, increased cAMP levels lead to downstream effects, and affected cells respond by increasing the enzyme that regulates cAMP activity (*3,4*). This regulation occurs through a negative feedback loop: increased cAMP stimulates protein kinase A (PKA), which in turn phosphorylates and activates phosphodiesterase (PDE) enzymes (*5*). PDEs then metabolize cAMP to its inactive form, thereby terminating the signal. PDE4 is the major subtype of PDE that metabolizes cAMP in brain and in some peripheral organs (*6,7*). Previous *in vitro* studies found increased cAMP activity in mouse models of fibrous dysplasia as well as in primary cultures of bone cells from individuals with MAS (*8-10*); however, to date, this relationship has not been demonstrated in humans *in vivo*.

In addition to fibrous dysplasia and endocrinopathies, neuropsychiatric impairments such as intellectual disability, anxiety, and attentional deficits are also found in some individuals with

MAS (*11*). Increased cAMP signaling could potentially be responsible for these findings, given the important role of cAMP signaling in the brain and the possibility that it could harbor *GNAS* mutations. Mouse models of analogous *GNAS* mutations in various brain regions demonstrated a potential link between activation of this pathway and various neuropsychiatric phenotypes (*12-15*). Nevertheless, the impact of the $G_s\alpha$ mutation on brain cAMP activity in individuals with MAS also remains unknown.

Notably, the positron emission tomography (PET) tracer ^{11}C-(*R*)-rolipram can be used to measure cAMP activity in humans. Rolipram is a reversible PDE4 inhibitor, and rolipram binding to PDE4 has been shown to increase with phosphorylation, meaning that ^{11}C-(*R*)-rolipram provides a measure of activity as well as density (*16,17*). In this context, ^{11}C-(*R*)-rolipram binding indirectly reflects cAMP activity; that is, increased cAMP signaling increases ^{11}C-(*R*)-rolipram binding.

This study investigated whether ^{11}C-(*R*)-rolipram binding is increased in dysplastic bone, brain, and/or peripheral organs. To achieve this, brain and whole-body PET scans with ^{11}C-(*R*)-rolipram were performed in both healthy controls and participants with MAS.

MATERIALS AND METHODS

Radioligand preparation

^{11}C-(*R*)-rolipram was labeled by ^{11}C-methylation of (*R*)-desmethyl-rolipram as previously described (*18*). The radioligand exhibited a high radiochemical purity (>99%) and had a molar activity of 87.45 ± 47.22 GBq/μmol at the time of injection (n = 22 batches).

Participants

This study (NCT02743377) was approved by the Institutional Review Board of the National Institute of Mental Health and Radiation Safety Committee of the National Institutes of Health. All participants provided written informed consent.

Six individuals with MAS and nine healthy controls between the ages of 18 and 55 participated in the study (see Table 1 for demographic characteristics). Of the six individuals with MAS, two had a clear neuropsychiatric phenotype (Table 2). Healthy controls were group-matched for age and sex and had no history of any major psychiatric or neurological disorder, as well as no current substance use disorder. All participants underwent a medical history, physical examination, analysis of blood chemistries, EKG, and a pregnancy test for women of child-bearing age.

^{11}C-(*R*)-rolipram whole-body and brain PET scans were performed in six individuals with MAS (six had whole-body scans and three had brain scans) and nine healthy controls (six had whole-body scans and seven had brain scans). All participants had a brain magnetic resonance imaging (MRI) scan and at least one PET scan (brain with arterial blood sampling and/or whole-body without arterial sampling) with ^{11}C-(*R*)-rolipram. Scans were completed within six months of initial evaluation for this study. Four of the individuals with MAS had a previous ^{18}F-NaF bone scan that was used to identify areas of active fibrous dysplasia.

Data acquisition

Whole-body and brain imaging: Whole-body and brain scans with ^{11}C-(*R*)-rolipram were performed as previously described (*19,20*). Prior to injection, computerized tomography scans were taken and used for attenuation correction. For both whole-body and brain scans, ^{11}C-(*R*)-

rolipram was injected intravenously over one minute, after which images were acquired for 120 and 90 minutes, respectively, with a Siemens Biograph mCT (Malvern, PA). For the brain scans (three for individuals with MAS, seven for healthy volunteers), arterial blood was sampled throughout the entire scan, with larger samples (2 – 6 mL) taken at specific time points for metabolite analysis and to measure plasma free fraction (f_P). A high-resolution 3T MRI was obtained for all participants.

Calculation of ^{11}C-(R)-Rolipram binding in whole body: The outcome measure used to calculate ^{11}C-(*R*)-rolipram binding in peripheral organs and bone was standardized uptake value (SUV), which is the concentration of radioactivity normalized to injected activity and body mass. The following organs were analyzed: the liver, gallbladder, bladder, lungs, spine, spleen, kidneys, stomach, and heart, as well as dysplastic bone (including the skull). For the latter, participant-specific ^{18}F-NaF PET/CT scans were reviewed for areas of active fibrous dysplasia, identified by its typical "ground glass" appearance and radiotracer uptake (Supplemental Figure S1). Corresponding bone regions were also drawn on scans from healthy controls.

Calculation of ^{11}C-(R)-Rolipram binding in brain: The outcome measure used to calculate ^{11}C-(*R*)-rolipram uptake in the brain was total distribution volume (V_T). V_T was measured in 12 predefined regions: frontal cortex, temporal cortex, parietal cortex, occipital cortex, hippocampus, thalamus, striatum, cingulate, amygdala, globus pallidus, insula, and cerebellum. Regions were generated from the participant-specific MRI, which were then co-registered to the PET scan. Two of the MAS participants had fibrous dysplasia on one side of the skull; to determine whether this affected ^{11}C-(*R*)-rolipram uptake, right - left differences in each region

were also investigated. Partial volume correction was also performed to determine whether brain deformations present in two of the MAS participants affected V_T.

Statistical analysis

Differences in age, gender, injected activity, molar activity, and mass dose were calculated using Student's *t*-tests. Differences in ^{11}C-(*R*)-rolipram uptake in organs were calculated using one-way analysis of variance (ANOVA).

RESULTS

Whole-body scans with ^{11}C-(*R*)-rolipram were performed in six healthy controls and six individuals with MAS. One of the healthy control scans was stopped early at approximately 60 minutes post-injection because the participant had a panic attack. Brain scans with ^{11}C-(*R*)-Rolipram and full arterial sampling were performed in eight healthy controls and three individuals with MAS. For one of the healthy control scans, however, an arterial line failure occurred 15 minutes post-injection, and the data were thus not used for this study. Sex, injected activity, molar activity, and mass dose did not differ between groups (Table 1). Although the age of the MAS participants (39 ± 2 years) was greater (P = 0.025) than that of the controls (28 ±3), no studies have reported that age affects ^{11}C-(*R*)-rolipram binding.

^{11}C-(R)-Rolipram identified dysplastic bone

^{11}C-(*R*)-rolipram uptake was higher in bones affected by fibrous dysplasia compared to both the unaffected bones of individuals with MAS and the same bones in healthy controls (Figures 1 and 2). In all four MAS participants who had a previously acquired ^{18}F-NaF bone scan for clinical purposes, ^{11}C-(*R*)-rolipram uptake colocalized with increased remodeling seen on the bone scan for most but not all regions (Figure 1). The ^{18}F-NaF bone scans were acquired 11 ± 13

months (range 0 – 29 months) prior to the PET rolipram scan in the four MAS participants who had a bone scan.

To assess uptake in peripheral organs, we measured the area-under-the-curve (AUC) of the concentration of radioactivity versus time from 30 to 120 minutes versus concentration of radioactivity: $AUC_{30\text{-}120}$ (SUV · min). The latter portions of the time activity curve were used because earlier intervals (e.g., 0 – 30 min) are strongly affected by blood flow to the organ. The $AUC_{30\text{-}120}$ of eight organs did not differ significantly between MAS participants and healthy controls (Supplemental Table S1). Because endocrine abnormalities are common in MAS, the thyroid and adrenal gland were visually examined and, similarly to healthy controls, both appeared normal in size on the CT image, with little ^{11}C-(*R*)-rolipram uptake.

No evidence of mosaicism in brains of MAS participants

Brain uptake of ^{11}C-(*R*)-rolipram was visually similar in MAS participants and healthy controls; that is, the uptake was fairly uniform, and no brain region was clearly elevated in MAS participants, regardless of whether or not they had neuropsychiatric symptoms. To highlight potential regional differences, uptake was normalized in each participant to the global average in that participant; again, no regional differences were apparent on visual inspection. To determine whether a global change might have occurred in MAS participants and healthy controls, uptake (as V_T) was also analyzed, and no global or regional differences were observed (Figure 3). V_T was chosen as the outcome measure instead of V_T/f_P (V_T corrected for the free fraction, f_P) because the sample size of this study was too small to determine whether f_P was stable within groups; thus, it was not included in order to reduce noise in the data. In addition, uptake for each region did not differ between the left and right hemispheres (data not shown). For the MAS participants who had extensive craniofacial involvement and compressed brain deformation,

partial volume correction had no impact on V_T (Supplemental Figure S2). As a result, partial volume correction was not included in the analysis so as to not increase noise in the data.

DISCUSSION

This study, which sought to assess whether ^{11}C-(*R*)-rolipram binding was increased in dysplastic bone and in peripheral organs of individuals with MAS versus healthy controls, had two major findings. First, ^{11}C-(*R*)-rolipram binding was increased in dysplastic bone, but not in other peripheral organs, as shown by whole-body scans. Second, ^{11}C-(*R*)-rolipram binding was not increased in the brains of individuals with MAS compared to healthy controls, and mosaicism (i.e., small areas of increased binding) was not apparent on visible inspection of the images.

In most radioligand binding studies using PET, increased uptake is caused by an increased density of the receptor/enzyme. For PDE4, however, binding of ^{11}C-(*R*)-rolipram may also reflect higher affinity of the enzyme for the radioligand. This is due to PKA-mediated phosphorylation of PDE4, which results not only in increased affinity for radioligand binding, but also in greater enzymatic activity (*21,22*). Consistent with this action of PKA, a previous study from our laboratory found that local injections of PKA modulators in rat brain had the expected effect on ^{11}C-(*R*)-rolipram binding, namely that activators increased radioligand binding and inhibitors decreased binding (*16,17*).

cAMP modulates its own activity through a negative feedback loop via two routes. The first route occurs quickly: increased cAMP activates PKA, which phosphorylates and activates PDE4, which then metabolizes cAMP (*5*). The second route occurs more slowly: prolonged PKA activation leads to phosphorylation of cAMP response element-binding protein (CREB), which then increases the translation of PDE4 mRNA (*23-26*). In this context, ^{11}C-(*R*)-rolipram binding

can be increased by both PKA-mediated phosphorylation of PDE4 as well as by increased synthesis of the enzyme. Both likely occur in dysplastic bone, as increased cAMP levels have been found in affected cells isolated *in vitro* from individuals with MAS (*27-29*). In fact, both routes probably occurred in our previous study, which measured ^{11}C-(*R*)-rolipram binding in individuals with major depressive disorder. In that study, PDE4 activity was decreased compared to controls but increased after two months of treatment with a selective serotonin reuptake inhibitor (*30*). Thus, it is reasonable to conclude that ^{11}C-(*R*)-rolipram binding reflects cAMP activity; nevertheless, that study could not determine whether the observed increases in ^{11}C-(*R*)-rolipram binding were due to increased phosphorylation of PDE4, to increased gene transcription, or to both.

In the present study, the areas of skeletal uptake seen on the PDE4 whole-body images coincided with areas of uptake seen in images from previously collected ^{18}F-NaF PET/CT scans. Increased cAMP signaling leads to dysplastic bone by the abnormal function formation of osteoblasts and osteoclasts —that is, cells responsible for bone remodeling. ^{18}F-NaF, which binds to the crystal surface of exposed bone, can be used to measure bone remodeling; higher binding indicates active remodeling, which underlies bone disorders like fibrous dysplasia (*31*). In this study, the ^{18}F-NaF and ^{11}C-(*R*)-rolipram images of the same MAS participants showed a high degree of concordance, indicating that increased cAMP activity was colocalized with areas of active fibrous dysplasia bone remodeling (Figure 1).

To be clear, we do not have definitive evidence that increased uptake of ^{11}C-(*R*)-rolipram in dysplastic bone reflects binding to PDE4. Nevertheless, increased specific binding is the most likely explanation for two reasons. First, if the effect was merely due to increased blood flow, the organ would have both a faster uptake and a faster washout. Instead, dysplastic bone had a

delayed peak and a slow washout (Figure 2), consistent with high affinity binding to a target that slows washout from the organ. Second, *in vitro* analyses of affected tissue have shown elevated concentration of cAMP and of PDEs. Thus, the mutation has two effects: increases the density of the target protein and increases the affinity for the radioligand via PKA-mediated phosphorylation. Arguably, the best evidence for specific binding would be a displacement study with a clinically approved PDE4 inhibitor, such as roflumilast. We explored this possibility during the conduct of this study, but we felt it would be unsafe. Based upon doses and plasma concentration in animals, the necessary human dose would 10-100 fold higher than that associated with severe nausea and vomiting.

PET radioligands can provide excellent pharmacological selectivity for the intended target; for example, ^{11}C-(*R*)-rolipram reflects binding to PDE4, but not to other PDEs (specifically, PDE1 through PDE11) (*32*). However, the anatomic resolution of PET is limited to about 2-4 mm. Thus, small changes can be overlooked if the signal is below the limit of detection, or if it is diluted by a surrounding and larger unaffected region. In fact, this error—called the partial volume effect—likely occurred in the current study. In endocrine organs, increased cAMP activity has been found to lead to disorders such as hyperthyroidism in MAS (*33*), but no such changes were detected with PET imaging in the current study. In fact, the same may be true of brain. The prevalence of neuropsychiatric disorders in MAS led us to hypothesize that cAMP mosaicism in the brain would mimic that in the periphery. However, one possible reason for these results, outside of the limitations of this study, is that the $G_s\alpha$ mutation did not affect the central nervous system of these MAS participants. Negative results could also be due to a type II error, meaning that while differences in brain uptake could be detected, it is likely that our methods were not sensitive enough. Possible explanations for the lack of sensitivity are

that the study had too few MAS participants; that only two had any neuropsychiatric symptoms; and that abnormalities in smaller brain regions could not be detected by the low resolution of the PET scan.

Conclusion

Whole body and brain PET scans were performed with the PDE4 radiotracer ^{11}C-(*R*)-rolipram in individuals with MAS and healthy controls. Increased ^{11}C-(*R*)-rolipram binding was found in dysplastic bone but not in other peripheral organs. No visual evidence of mosaicism was observed in brain, but small regions may not be detectable by the relatively low resolution of PET. This study is the first to confirm that ^{11}C-(*R*)-rolipram, a radiolabeled inhibitor of PDE4, can measure the known increases in cAMP activity *in vivo* found in MAS. In addition, this study supports the utility of such PET scans to indirectly measure altered cAMP signaling in other human diseases, including major depressive disorder, if the abnormality extends to adequately-sized regions of the target organ.

FINANCIAL DISCLOSURES

This study was funded by the Intramural Research Programs of the National Institute of Mental Health (ZIAMH002852 and ZIAMH002793) and the National Institute of Dental and Craniofacial Research (ZIADE000649), National Institutes of Health.

CONFLICT OF INTEREST

The authors have no conflicts of interest to disclose, financial or otherwise.

ACKNOWLEDGEMENTS

The authors are grateful to the staff of Molecular Imaging Branch for subject recruitment; to the NIH's PET Department (Chief: Peter Herscovitch, MD) for performing the PET scans; and to Ioline Henter for invaluable editorial assistance.

KEY POINTS

Question: This study sought to determine whether ^{11}C-(*R*)-rolipram binding could detect the expected increased cyclic adenosine monophosphate (cAMP) signaling in dysplastic bone of individuals with McCune Albright Syndrome (MAS), a rare genetic mosaic disorder associated with excessive production of cAMP; rolipram is a reversible inhibitor of phosphodiesterase-4 (PDE4).

Pertinent Findings: ^{11}C-(*R*)-rolipram identified areas of dysplastic bone in individuals with MAS but did not visualize increased uptake in any other organ, some of which presumably had small areas of increased cAMP signaling.

Implications for Patient Care: These findings have no direct implications for clinical care; instead, they provide pathophysiological knowledge from living participants of the presence of increased cAMP signaling in affected areas of bone.

REFERENCES

1. Weinstein LS, Shenker A, Gejman PV, Merino MJ, Friedman E, Spiegel AM. Activating mutations of the stimulatory G protein in the McCune-Albright syndrome. *N Engl J Med.* 1991;325:1688-1695.

2. Boyce AM, Florenzano P, de Castro LF, Collins MT. Fibrous Dysplasia/McCune-Albright Syndrome. In: Adam MP, Ardinger HH, Pagon RA, et al., eds. *GeneReviews((R))*. Seattle (WA); 1993.

3. Mehats C, Andersen CB, Filopanti M, Jin S-LC, Conti M. Cyclic nucleotide phosphodiesterases and their role in endocrine cell signaling. *Trends Endocrin Met.* 2002;13:29-35.

4. Nemoz G, Sette C, Hess M, Muca C, Vallar L, Conti M. Activation of Cyclic Nucleotide Phosphodiesterases in FRTL-5 Thyroid Cells Expressing a Constitutively Active Gsalpha. *Mol Endocrinol.* 1995;9:1279-1287.

5. Houslay MD, Adams DR. PDE4 cAMP phosphodiesterases : modular enzymes that orchestrate signalling cross-talk, desensitization and compartmentalization. *Biochem J.* 2003;370:1-18.

6. Houslay MD, Sullivan M, Bolger GB. The multienzyme PDE4 cyclic adenosine monophosphate-specific phosphodiesterase family: intracellular targeting, regulation, and selective inhibition by compounds exerting anti-inflammatory and antidepressant actions. *Adv Pharmacol.* 1998;44:225-342.

7. Richter W, Menniti FS, Zhang HT, Conti M. PDE4 as a target for cognition enhancement. *Expert Opin Ther Targets.* 2013;17:1011-1027.

8. Hsiao EC, Boudignon BM, Chang WC, et al. Osteoblast expression of an engineered Gs-coupled receptor dramatically increases bone mass. *Proc Natl Acad Sci U S A.* 2007;105:1209-1214.

9. Palmisano B, Spica E, Remoli C, et al. RANKL inhibition in fibrous dysplasia of bone: a preclinical study in a mouse model of the human disease. *J Bone Miner Res.* 2019;34:2171-2182.

10. Weinstein LS. G(s)alpha mutations in fibrous dysplasia and McCune-Albright syndrome. *J Bone Miner Res.* 2006;21 Suppl 2:P120-124.

11. Brown RJ, Kelly MH, Collins MT. Cushing syndrome in the McCune-Albright syndrome. *J Clin Endocrinol Metab.* 2010;95:1508-1515.

12. Bourtchouladze R, Patterson SL, Kelly MP, Kreibich A, Kandel ER, Abel T. Chronically increased Gsalpha signaling disrupts associative and spatial learning. *Learn Mem.* 2006;13:745-752.

13. Kelly MP, Cheung YF, Favilla C, et al. Constitutive activation of the G-protein subunit Galphas within forebrain neurons causes PKA-dependent alterations in fear conditioning and cortical Arc mRNA expression. *Learn Mem.* 2008;15:75-83.

14. Kelly MP, Isiegas C, Cheung YF, et al. Constitutive activation of Galphas within forebrain neurons causes deficits in sensorimotor gating because of PKA-dependent decreases in cAMP. *Neuropsychopharmacology.* 2007;32:577-588.

15. Kelly MP, Stein JM, Vecsey CG, et al. Developmental etiology for neuroanatomical and cognitive deficits in mice overexpressing Galphas, a G-protein subunit genetically linked to schizophrenia. *Mol Psychiatry.* 2009;14:398-415, 347.

16. Itoh T, Abe K, Hong J, et al. Effects of cAMP-dependent protein kinase activator and inhibitor on in vivo rolipram binding to phosphodiesterase 4 in conscious rats. *Synapse.* 2010;64:172-176.

17. Itoh T, Abe K, Zoghbi SS, et al. PET measurement of the in vivo affinity of 11C-(R)-rolipram and the density of its target, phosphodiesterase-4, in the brains of conscious and anesthetized rats. *J Nucl Med.* 2009;50:749-756.

18. Fujita M, Zoghbi SS, Crescenzo MS, et al. Quantification of brain phosphodiesterase 4 in rat with (R)-[11C]Rolipram-PET. *Neuroimage.* 2005;26:1201-1210.

19. Fujita M, Hines CS, Zoghbi SS, et al. Downregulation of brain phosphodiesterase type IV measured with 11C-(R)-rolipram positron emission tomography in major depressive disorder. *Biol Psychiatry.* 2012;72:548-554.

20. Lohith TG, Zoghbi SS, Morse CL, et al. Brain and whole-body imaging of nociceptin/orphanin FQ peptide receptor in humans using the PET ligand 11C-NOP-1A. *J Nucl Med.* 2012;53:385-392.

21. Hoffmann R, Wilkinson IR, McCallum JF, Engels P, Houslay MD. cAMP-specific phosphodiesterase HSPDE4D3 mutants which mimic activation and changes in rolipram inhibition triggered by protein kinase A phosphorylation of Ser-54 : generation of a molecular model. *Biochem J.* 1998;333:139-149.

22. Zanotti-Fregonara P, Zoghbi SS, Liow JS, et al. Kinetic analysis in human brain of [11C](R)-rolipram, a positron emission tomographic radioligand to image phosphodiesterase 4: a retest study and use of an image-derived input function. *Neuroimage.* 2011;54:1903-1909.

23. Conti M, Beavo J. Biochemistry and physiology of cyclic nucleotide phosphodiesterases: essential components in cyclic nucleotide signaling. *Annu Rev Biochem.* 2007;76:481-511.

24. Conti M, Jin S-LC, Monaco L, Repaske DR, Swinnen JV. Hormonal regulation of cyclic nucleotide phosphodiesterases. *Endocin Rev.* 1991;12:218-233.

25. Conti M, Richter W, Mehats C, Livera G, Park JY, Jin C. Cyclic AMP-specific PDE4 phosphodiesterases as critical components of cyclic AMP signaling. *J Biol Chem.* 2003;278:5493-5496.

26. Sette C, Conti M. Phosphorylation and activation of a cAMP-specific phosphodiesterase by the cAMP-dependent protein kinase. *J Biol Chem.* 1996;271:16526-16534.

27. Marie PJ, de Pollak C, Chanson P, Lomri A. Increased proliferation of osteoblastic cells expressing the activating Gs alpha mutation in monostotic and polyostotic fibrous dysplasia. *Am J Pathol.* 1997;150:1059-1069.

28. Sette C, Vicini E, Conti M. Modulation of cellular responses by hormones: role of CAMP specific, rolipram-sensitive phosphodiesterases. *Mol Cell Endorinol.* 1994;100:75-79.

29. Yamamoto T, Ozono K, Kasayama S, et al. Increased IL-6 production by cells isolated from the fibrous bone dysplasia tissues in patients with McCune-Albright syndrome. *J Clin Invest.* 1996;98:30-35.

30. Fujita M, Richards EM, Niciu MJ, et al. cAMP signaling in brain is decreased in unmedicated depressed patients and increased by treatment with a selective serotonin reuptake inhibitor. *Mol Psychiatry.* 2017;22:754-759.

31. Papadakis G, Manikis G, Karantanas A, et al. (18) F-N aF PET/CT imaging in fibrous dysplasia of bone. *J Bone Miner Res.* 2019;34:1619-1631.

32. Schneider HH, Schmiechen R, Brezinski M, Seidler J. Stereospecific binding of the antidepressant rolipram to brain protein structures. *Eur J Pharm.* 1986;127:105-115.

33. Robinson C, Collins MT, Boyce AM. Fibrous Dysplasia/McCune-Albright Syndrome: clinical and translational perspectives. *Curr Osteoporos Rep.* 2016;14:178-186.

34. Collins MT, Kushner H, Reynolds JC, et al. An instrument to measure skeletal burden and predict functional outcome in fibrous dysplasia of bone. *J Bone Miner Res.* 2005;20:219-226.

TABLES

Table 1. Participant Demographics

	Healthy Controls (n=9, 13 scans)	MAS (n=6, 9 scans)	p-value
Age	28 ± 3.4	39 ± 2	0.025
Proportion Female	78%	83%	
Injected Activity (MBq)	708 ± 61	725 ± 84	0.61
Molar Activity (kBq/nmol)	60 ± 24	81 ± 41	0.15
Mass Dose (nmol/kg)	0.19 ± 0.1	0.19 ± 0.1	0.99

MAS = McCune-Albright syndrome

Table 2. Clinical Characteristics of MAS Participants

	Age/Race/Sex	Scan type	MAS endocrinopathies	Neuropsychiatric disorder	Fibrous dysplasia locations	Skeletal Burden Score[1]
MAS #1	34 WF	Whole body, Brain	History of precocious puberty, hyperthyroidism	Major depressive disorder	Cf, Ax, Ap	61
MAS #2	20 WF	Whole body	None	Depression, mild cognitive impairment, schizophrenia/schizoaffective disorder, anxiety	Cf	7
MAS #3	55 WF	Whole body, Brain	Growth hormone excess	None	Cf, Ax, Ap	18
MAS #4	47 WF	Whole body, Brain	History of precocious puberty	None	Cf, Ax	3
MAS #5	33 WM	Whole body	Growth hormone excess, hyperthyroidism	None	Cf, Ax, Ap	75
MAS #6	44 WF	Whole body	History of precocious puberty, hyperthyroidism	None	Cf, Ax, Ap	36

W = white, F = female, M = male, MAS = McCune-Albright syndrome, Cf = craniofacial skeleton, Ax = axillary skeleton, Ap = appendicular skeleton. [1]Validated tool for quantifying fibrous dysplasia involvement (see (*34*))

FIGURES

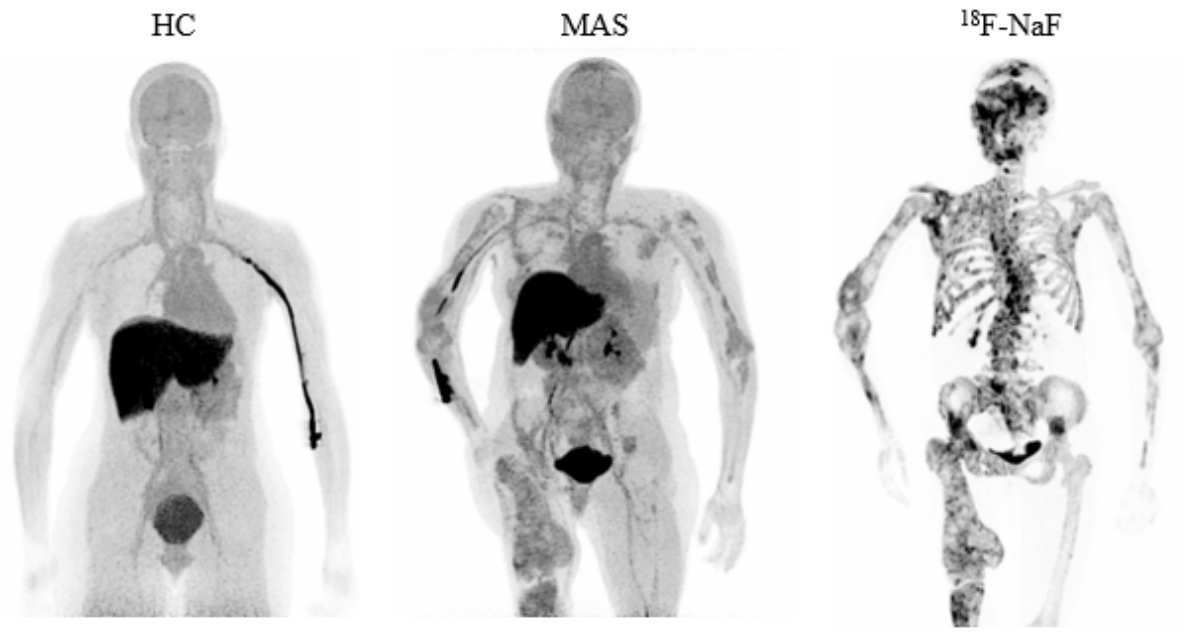

Figure 1. ^{11}C-(*R*)-Rolipram binding was colocalized with dysplastic bone in individuals with McCune-Albright Syndrome (MAS). Maximum intensity projections (MIP) of ^{11}C-(*R*)-rolipram standardized uptake value (SUV) (averaged 10-30 minutes, five frames) are shown in a representative healthy control (HC, left) and MAS participant #1 (middle), as well as an ^{18}F-NaF PET/CT scan of MAS participant #1 within one year of ^{11}C-(*R*)-rolipram scan (right). An MIP image projects the voxels with maximum intensity in the visualization plane onto a 2D image.

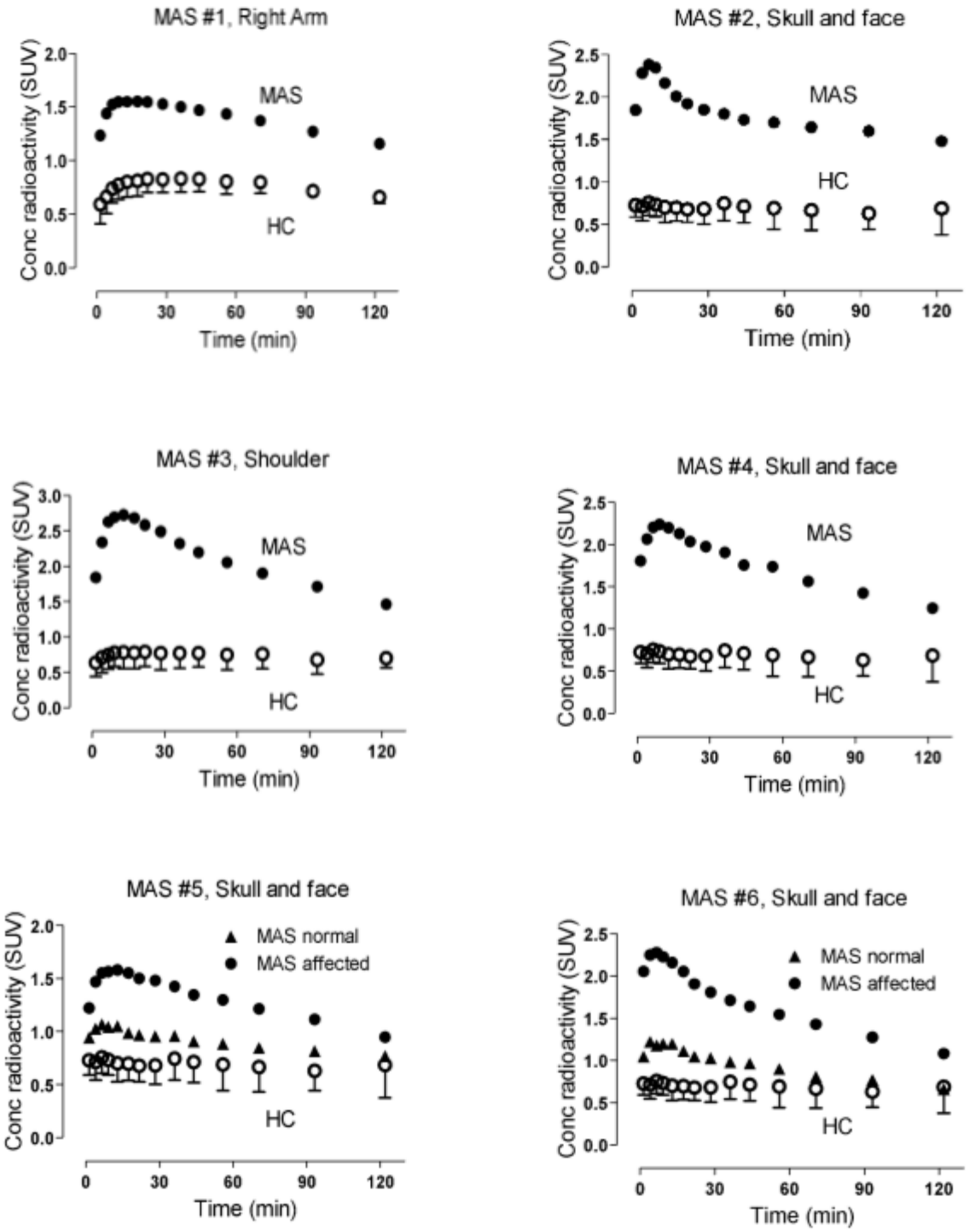

Figure 2. ^{11}C-(*R*)-rolipram uptake was higher in areas of fibrous dysplasia (black circles) compared to healthy controls (white circles). Specific regions were drawn for each McCune-

Albright Syndrome (MAS) participant depending on the location of the dysplastic bone. In some MAS participants, dysplastic lesions were localized on one side, and dysplastic lesions were compared to normal lesions in the same participants (black triangles). SUV = standardized uptake value. The error bars show SDs.

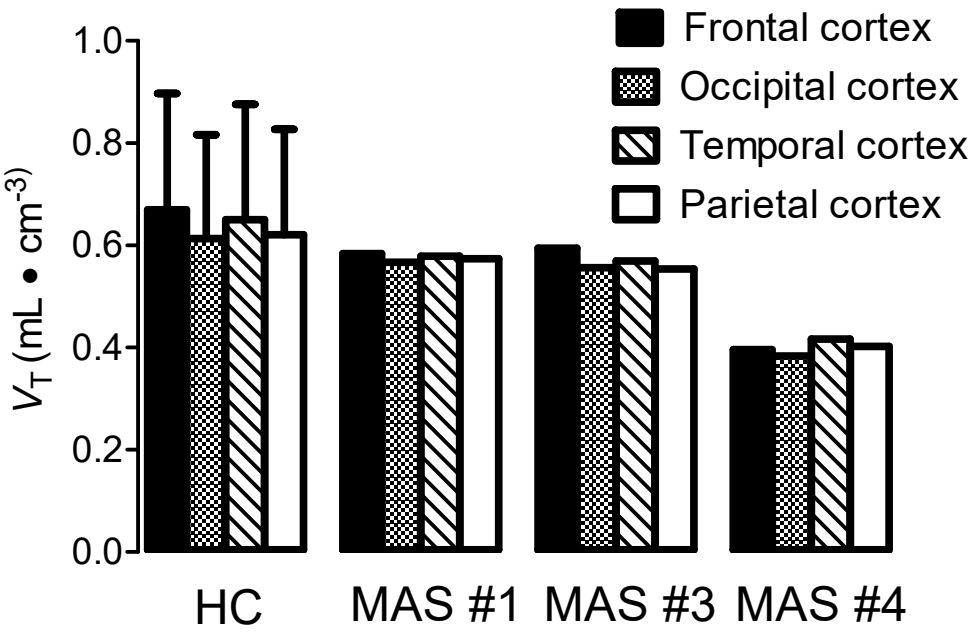

Figure 3. No evidence of mosaicism was observed in different brain regions of participants with McCune-Albright Syndrome (MAS). ^{11}C-(*R*)-rolipram uptake in the brain, measured as total distribution volume (V_T), was unchanged across brain regions in both healthy controls (HCs) and individuals with MAS. The error bars show SDs.

SUPPLEMENTAL MATERIALS

Supplemental Table S1. Organ uptake of ^{11}C-(*R*)-rolipram in MAS participants and healthy controls

Organ	AUC_{30-120} (SUV · min)		p value
	MAS Participants	Controls	
Bladder	650.8 ± 344.7	575.1 ± 402.2	0.784
Gallbladder	417.9 ± 317.8	581.2 ± 235.8	0.467
Heart	25.4 ± 5.8	27.4 ± 6.1	0.640
Kidneys	80.4 ± 12.4	63.3 ± 14.8	0.128
Liver	52.4 ± 4.4	47.6 ± 21.7	0.682
Lungs	9.6 ± 4.4	10.2 ± 4.3	0.851
Spleen	18.7 ± 2.7	20.1 ± 2.8	0.510
Stomach	34.1 ± 22.8	39.4 ± 20.8	0.742

MAS = McCune-Albright syndrome; SUV = standardized uptake value;
AUC_{30-120} (SUV · min) = the area-under-the-curve of the concentration of radioactivity vs time from 30 to 120 minutes versus concentration of radioactivity.

Supplemental Figure S1

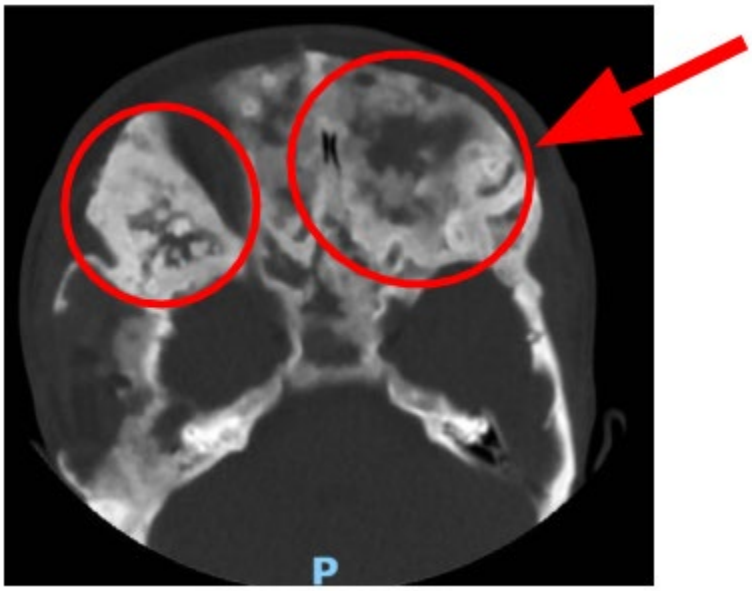

Supplemental Figure S1. Example CT cross section of McCune-Albright Syndrome (MAS) participant #1 showing areas of fibrous dysplasia.

Supplemental Figure S2

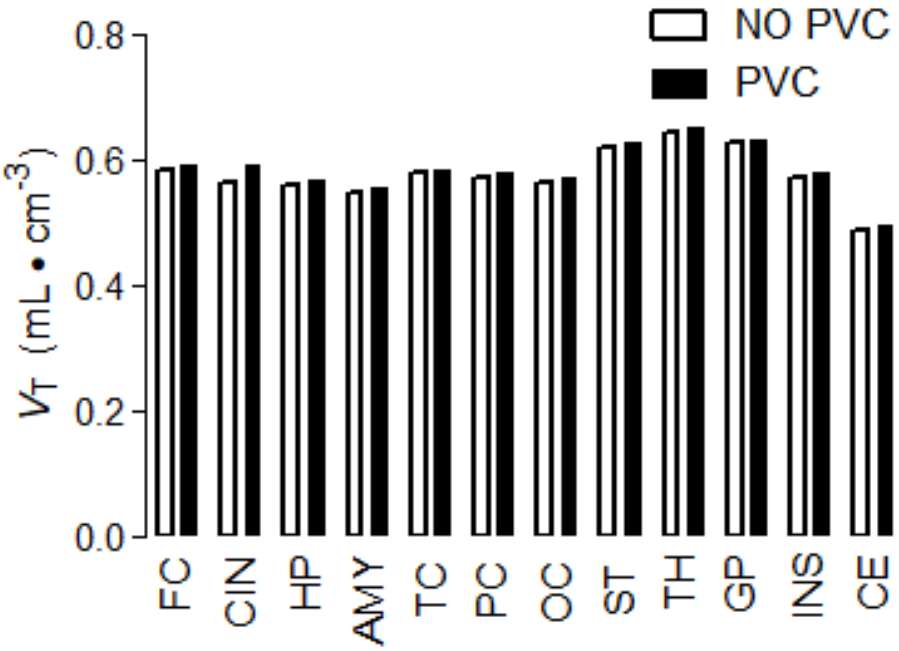

Supplemental Figure S2. The distribution volume (V_T) of ^{11}C-(*R*)-rolipram in twelve brain regions was the same with (black) and without (white) partial volume correction (PVC). FC = frontal cortex; CIN = cingulate; HP = hippocampus, AMY = amygdala; TC = temporal cortex; PC = parietal cortex; OC = occipital cortex: ST = striatum; TH = thalamus; GP = globus pallidus; INS = insula; CE = cerebellum.